

# Real-time observation of DNA translocation by the type I restriction modification enzyme *EcoR124I*

Ralf Seidel<sup>1</sup>, John van Noort<sup>1,3</sup>, Carsten van der Scheer<sup>1</sup>, Joost G P Bloom<sup>1</sup>, Nynke H Dekker<sup>1</sup>, Christina F Dutta<sup>2</sup>, Alex Blundell<sup>2</sup>, Terence Robinson<sup>2</sup>, Keith Firman<sup>2</sup> & Cees Dekker<sup>1</sup>

**Type I restriction enzymes bind sequence-specifically to unmodified DNA and subsequently pull the adjacent DNA toward themselves. Cleavage then occurs remotely from the recognition site. The mechanism by which these members of the superfamily 2 (SF2) of helicases translocate DNA is largely unknown. We report the first single-molecule study of DNA translocation by the type I restriction enzyme *EcoR124I*. Mechanochemical parameters such as the translocation rate and processivity, and their dependence on force and ATP concentration, are presented. We show that the two motor subunits of *EcoR124I* work independently. By using torsionally constrained DNA molecules, we found that the enzyme tracks along the helical pitch of the DNA molecule. This assay may be directly applicable to investigating the tracking of other DNA-translocating motors along their DNA templates.**

Translocation of enzymes along DNA, driven by molecular motors, plays a crucial role during many vital DNA-processing steps in the cellular cycle, including repair, recombination, replication, transcription and restriction. In the past, several DNA-translocating enzymes have been thoroughly studied. In comparison to classical motor proteins such as kinesin and myosin, however, the translocation properties of a variety of DNA enzymes are still inadequately characterized and therefore a subject of current research<sup>1–4</sup>. Until now, very different mechanistic models have been postulated even for closely related enzymes that share conserved amino acid sequence motifs, for example helicases<sup>5</sup>. For a comprehensive understanding of the motor function, it is necessary to probe the dynamics of the system and gain essential knowledge about the translocation rate, forces produced, dependence of the translocation on ATP concentration, processivity, termination and reinitiation of motor activity, coordination between different motors and torque generation. Here, we have used magnetic tweezers to directly address these questions, at the single-molecule level, for the type I restriction modification (R-M) enzyme *EcoR124I*.

In contrast to the type II R-M systems, type I systems accomplish DNA restriction and modification through a single enzyme<sup>6</sup>. This enzyme consists of a DNA methyltransferase core enzyme (MTase), which carries out sequence-specific DNA binding as well as target methylation, and two HsdR subunits, which conduct the restriction reaction. DNA restriction is dependent on the hydrolysis of ATP and occurs at random loci up to several thousands of base pairs (bp) away from the DNA-binding site<sup>7</sup>. After DNA binding, the MTase remains bound to the recognition site, whereas both HsdR subunits can

translocate the adjacent DNA in a bidirectional manner, thus pulling the DNA toward the bound complex. This results in the formation of two DNA loops<sup>8</sup> (Fig. 1a). Cleavage occurs upon collision of the translocating complex with a 'roadblock', such as a second restriction enzyme<sup>9,10</sup>. Although endonuclease and ATPase activity have been characterized in previous biochemical assays<sup>11,12</sup>, the actual translocation mechanism remains largely unclear.

Here, we show that the two motor subunits of *EcoR124I* are independent motors that translocate along the helical pitch of the DNA. In addition, we find a dynamic termination and reinitiation of translocation activity that is governed by disassembly and reassembly of the enzyme.

The investigation of the translocation process of *EcoR124I* is also of general importance to a better understanding of the mechanism of DNA translocation for other SF2 helicases, including DNA helicases, ATP-dependent chromatin remodeling factors and type III restriction enzymes<sup>13</sup>.

## RESULTS

### Assembly of the enzyme

For *EcoR124I*, in contrast to other type I restriction enzymes, the second HsdR unit is more weakly bound than the first<sup>14</sup>. Thus, depending on the ratio between HsdR and MTase, a complex carrying either a single motor subunit ( $R_1$ ) or two motor subunits ( $R_2$ ) can be formed (see Fig. 1a and Methods). Whereas the  $R_2$  complex cleaves DNA efficiently, the  $R_1$  complex is unable to carry out DNA cleavage<sup>14</sup>. This unique property of *EcoR124I* allows the study of single motor subunits as well as the fully assembled endonucleases.

<sup>1</sup>Kavli Institute of Nanoscience, Delft University of Technology, Lorentzweg 1, 2628 CJ Delft, The Netherlands. <sup>2</sup>IBBS Biophysics Laboratories, School of Biological Sciences, University of Portsmouth, St. Michael's Building, White Swan Road, Portsmouth PO1 2DT, UK. <sup>3</sup>Present address: Department of Biophysics, Huygens Laboratory, Leiden University, 2300 RA Leiden, The Netherlands. Correspondence should be addressed to R.S. (seidel@mb.tn.tudelft.nl).

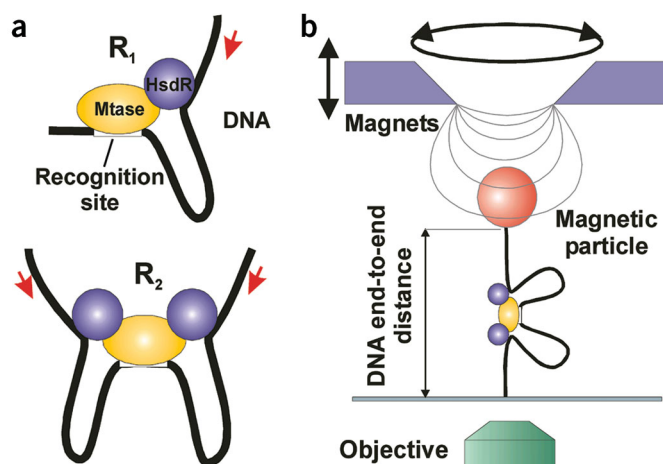


**Figure 1** Schematic drawings of the DNA–enzyme complexes and the experimental setup. (a) Schematic drawing of a type I restriction enzyme translocating DNA. While the MTase unit stays bound at the recognition site, the HsdR unit(s) pull in the DNA. This leads to the formation of DNA loops. For *EcoR124I*, a complex with one ( $R_1$ ) or with two motor units ( $R_2$ ) can be assembled depending on the HsdR/MTase ratio. (b) Schematic drawing of the magnetic tweezers setup. A DNA molecule is attached on one end to the bottom of the flow cell and at the other end to a magnetic bead. A pair of magnets is used to stretch and to supercoil the DNA. The DNA end-to-end distance is determined using video microscopy and image analysis.

### Complex with a single motor unit ( $R_1$ )

A magnetic tweezers setup<sup>15</sup> was used to monitor the end-to-end distance of a single DNA molecule bound at one end to a magnetic bead and at the other end to the surface of a flow cell (Fig. 1b). A pair of external magnets was used to stretch and supercoil the DNA molecule. When  $R_1$  complex was added to the flow cell containing DNA molecules with a single *EcoR124I* recognition site in the presence of ATP, characteristic repeatable events occurred during which the DNA end-to-end distance decreased (Fig. 2a). This is expected for the translocation of *EcoR124I*, because it pulls in the DNA and forms DNA loops (Fig. 1). No such events were observed when using (i) nonhydrolyzable ATP- $\gamma$ S (ii) DNA without a recognition site or (iii) neither ATP nor enzyme (data not shown). A single event, which we attribute to DNA translocation by *EcoR124I*, is characterized by the initiation of translocation, then processive translocation at a constant rate; the event is terminated by dissociation of the enzyme (Fig. 2b).

Many events were fitted to extract the translocation rate and the event duration (see Methods). The distribution of the measured translocation rate is quite narrow. For example, a mean of  $555 \text{ bp s}^{-1}$  and an s.d. of  $\sim 90 \text{ bp s}^{-1}$  are obtained at an applied force of  $0.8 \text{ pN}$  in the presence of  $4 \text{ mM}$  ATP (Fig. 2c, inset). This points to a common translocation process for all events. In particular, no events were observed at half or double the mean rate, which would indicate a

varying number of translocating subunits. To ascertain whether the observed translocation is due to a single HsdR unit, we compared a DNA construct with the recognition site  $>2 \text{ kilobases (kb)}$  from the bead (called construct I) with a construct with this site at  $275 \text{ bp}$  from the bead (called construct II) (Fig. 2a, inset). Construct I should allow long stretches of translocation in both directions, whereas construct II should confine translocation in the direction of the bead to only  $275 \text{ bp}$ . Very similar translocation rates were observed on both DNA constructs (Fig. 2c). In experiments with DNA construct II, a new type of event was observed, which we term stalling: the enzyme translocates for a short distance, then suddenly stops and rests at this position, before it finally dissociates (Fig. 3). No such stalling was observed using DNA construct I. Plotting the stalling position in a histogram resulted in a mean stalling distance of  $270 \pm 30 \text{ bp}$  (Fig. 3, inset), in agreement with the distance between the recognition site and the bead. This implies that enzyme translocation stalls at the magnetic bead.

These findings all confirm that a single translocating motor is the origin of the observed events. Otherwise no stalling events would be detected. The observed stalling events also indicate the direction of the translocation. Translocation occurs in both directions in an arbitrary order (Fig. 3); in other words, the enzyme can switch directions before it starts to translocate again.

No significant dependence of the translocation rate on force was observed up to  $4 \text{ pN}$  in the presence of  $4 \text{ mM}$  ATP (Fig. 2c). Higher

**Figure 2** Translocation of the  $R_1$  complex.

(a) Typical time trace of enzyme activity after addition of  $4 \text{ mM}$  ATP using DNA construct II. Inset: the two DNA constructs used in the magnetic tweezers. White box, *EcoR124I* recognition site. (b) Enlarged view of a single translocation event of a different time trace using the same DNA construct. (c) Averaged translocation rates as a function of force at  $4 \text{ mM}$  ATP. The average translocation rate over all forces is  $550 \pm 30 \text{ bp s}^{-1}$  as indicated by the line. Inset: histogram of the translocation rates measured at  $0.8 \text{ pN}$ . The mean translocation rate is  $555 \text{ bp s}^{-1}$  with an s.d. of  $90 \text{ bp s}^{-1}$ . (d) Averaged translocation rates versus ATP concentration. The data set is well fit by the Michaelis-Menten relation  $V_{\text{max}}[\text{ATP}] / ([\text{ATP}] + K_m)$ .

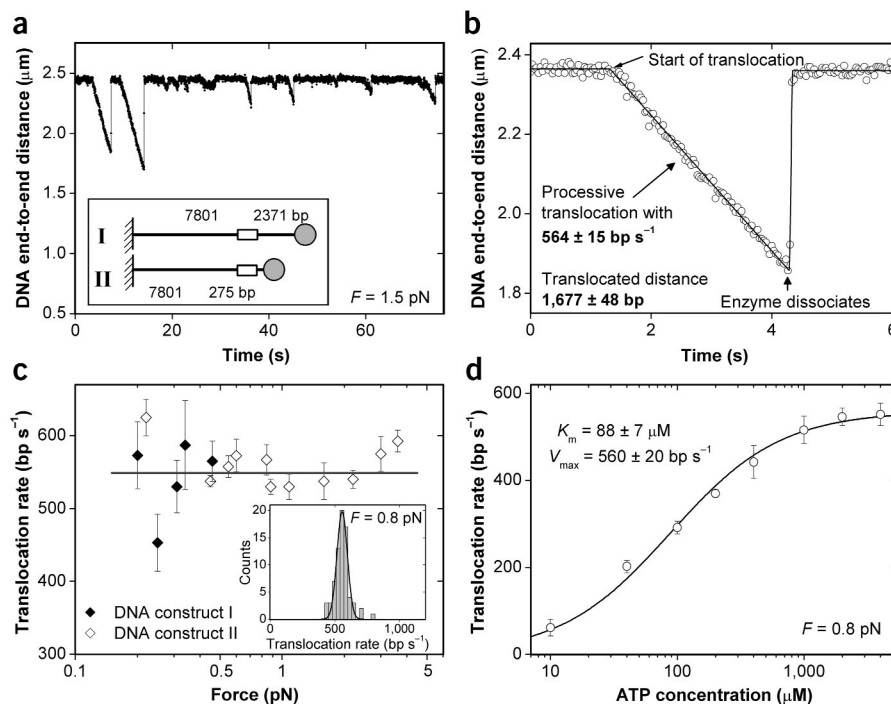
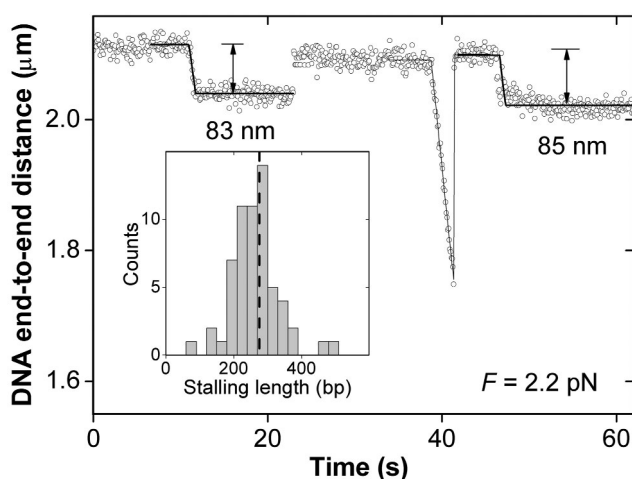


**Figure 3** Time trace with stalling events obtained with DNA construct II at 4 mM ATP. Inset: histogram of the stalling distance. The mean stalling position is  $270 \pm 30$  bp, in agreement with the distance of the bead from the recognition site of 275 bp, indicated by the dashed line. Thus, stalling is caused by the blocking of enzyme translocation at the magnetic bead.

forces could not be measured, because the processivity is too greatly reduced (see next section). The mean translocation rate  $\langle v \rangle$  of a single HsdR subunit, obtained by averaging over all measured forces, was found to be  $550 \pm 30$  bp  $s^{-1}$ . Because the measured translocation rate might depend on the actual ATP concentration, experiments were carried out with varying amounts of ATP in solution. The translocation rate changes with the ATP concentration in accordance with Michaelis-Menten kinetics, yielding a maximum translocation rate of  $V_{\max} = 560 \pm 20$  bp  $s^{-1}$  and  $K_m = 88 \pm 7$   $\mu$ M (Fig. 2d). Thus, the measurements at 4 mM ATP, reported here, correspond to saturating ATP conditions.

### Complex with two motor units ( $R_2$ )

A functional endonuclease with two motor units was obtained at an 8:1 ratio of HsdR to M $Tase^{14}$ . After addition of the reconstituted enzyme to the flow cell, translocation did not produce instantaneous DNA cleavage, which would result in a loss of the magnetic bead. Instead, several complicated translocation events were observed. These events lasted much longer than for the  $R_1$  complex, the translocation rate was not constant and termination of an event occurred in several substeps until the initial DNA end-to-end distance was reached (Fig. 4a). Closer evaluation of the time traces revealed subregions of constant speeds. In one example (Fig. 4b), after translocation starts, the speed suddenly increases, and after a while it abruptly decreases again. Translocation rates of all subregions with constant speed were determined by fitting them with a straight line. A histogram of the translocation rates yields two distinct peaks (Fig. 4c). One is centered at  $510 \pm 30$  bp  $s^{-1}$  and the other at  $990 \pm 30$  bp  $s^{-1}$ , which is, within experimental error, twice the rate of the first peak. We attribute this doubled translocation velocity to simultaneous activity of the two HsdR subunits. The different slopes apparent in the trace of Figure 4b can now be understood. Initially, a single motor was translocating; then the second motor started translocating, until one of the motors stalled but remained attached to the translocated DNA, while the other



HsdR subunit continued to translocate. If one calculates for the trace in Figure 4b the distance that each motor translocated until one of them stalled at  $\sim 6$  s, one finds that after the first motor had translocated  $1,400 \pm 100$  bp, there followed a period during which both motors traveled  $1,050 \pm 50$  bp simultaneously. Thus, in total one motor translocated  $2,450 \pm 150$  bp and the other one  $1,050 \pm 150$  bp. This strongly suggests that the observed stalling occurred at the magnetic bead, because the distance from the recognition site to the bead in this construct is 2,371 bp (DNA construct I). The occurrence of stalling can also be seen during dissociation of the enzyme, as in Figure 4a at  $\sim 40$  s. After dissociation of the first motor subunit, the second one remained stalled for some time at a distance of  $2,400 \pm 100$  bp. In fact, plotting the DNA end-to-end distances of all traces into a histogram results in a peak at  $2,440 \pm 90$  bp (data not shown). Notably, stalling did not necessarily lead to immediate cleavage, and beads were typically lost, indicating that cleavage finally occurred, only after several minutes when many stalling events had passed.

### Processivity

Processivity of the  $R_1$  complex carrying one motor subunit is greatly reduced compared with that of the fully assembled  $R_2$  complex with two motor subunits. For the  $R_1$  complex, a histogram of the event

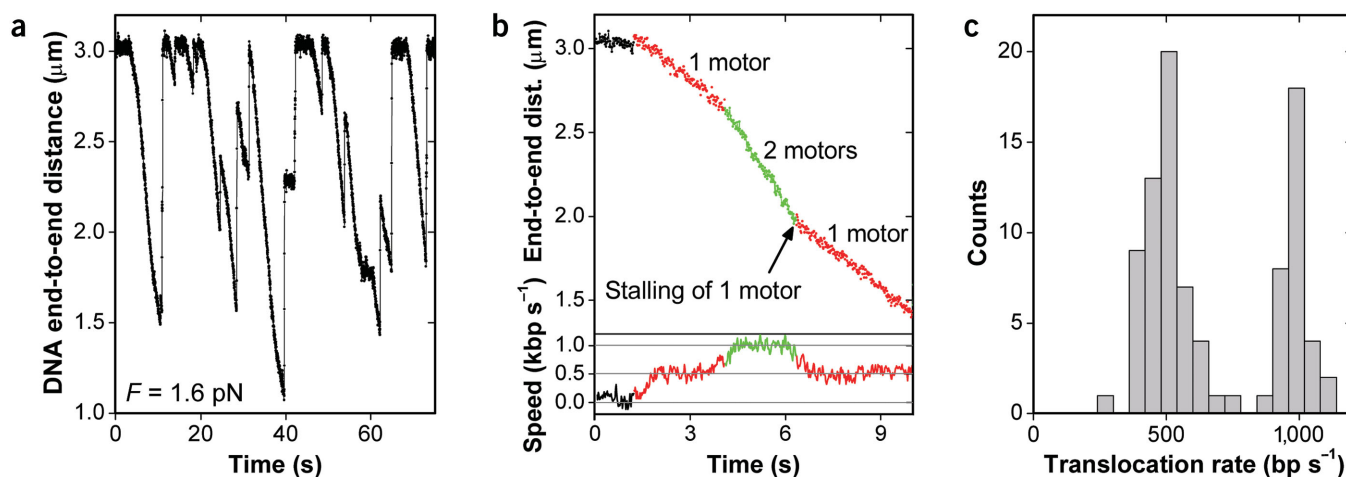


**Figure 4** Translocation of the  $R_2$  complex at 4 mM ATP. (a) Time trace obtained on DNA construct I. (b) Enlarged view on a time trace. The speed, denoted at the bottom, is the derivative of the time trace smoothed with a 1-Hz median filter. (c) Histogram of the translocation rates. The mean rates of the two peaks are  $510 \pm 30$  bp  $s^{-1}$  and  $990 \pm 30$  bp  $s^{-1}$ . Counts refer to the number of subregions with constant translocation rate.

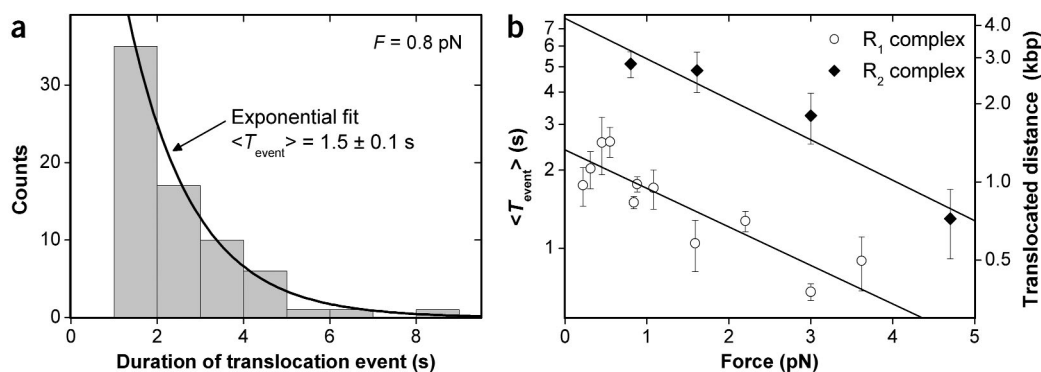


**Figure 5** (a) Histogram of the duration of single translocation events for the  $R_1$  complex measured at 0.8 pN and 4 mM ATP using construct II. Events of duration  $<180$  nm or  $<1$  s have not been considered, because they cannot be clearly distinguished from the noise of the movement of the magnetic bead. The translocation-time distribution decays exponentially, given by the mean event duration  $\langle T_{\text{event}} \rangle$ . (b) Dependence of  $\langle T_{\text{event}} \rangle$  on force measured for

the  $R_1$  and the  $R_2$  complex at 4 mM ATP. The right axis scale shows the corresponding mean translocated distance obtained by multiplication of  $\langle T_{\text{event}} \rangle$  by the mean translocation rate.  $\langle T_{\text{event}} \rangle$  at zero force is obtained by fitting the data with a force-dependent Arrhenius equation  $\langle T_{\text{event}} \rangle = \langle T_{\text{event}} \rangle_{F=0} \exp[-\delta F / kT]$ . Here, the parameter  $\delta$  corresponds to the distance the enzyme has to be displaced to induce detachment and termination of the translocation. For the  $R_1$  complex,  $\langle T_{\text{event}} \rangle_{F=0} = 2.4 \pm 0.3$  s,  $\delta = 1.4 \pm 0.3$  nm, and  $\langle L \rangle_{F=0} = 1,320 \pm 150$  bp. For the  $R_2$  complex,  $\langle T_{\text{event}} \rangle_{F=0} = 7.7 \pm 1.6$  s,  $\delta = 1.5 \pm 0.3$  nm, and  $\langle L \rangle_{F=0} = 4,300 \pm 900$  bp.

duration  $T_{\text{event}}$  of all events at a given force yields a distribution that decays exponentially (Fig. 5a). This points to first-order kinetics, governed by a single rate  $k_{\text{off}}$  for the dissociation of the enzyme that results in termination of DNA translocation. Fitting the histogram to an exponential results in a mean event time  $\langle T_{\text{event}} \rangle$  of  $1.5 \pm 0.1$  s, at 0.8 pN, which is by definition the inverse of the  $k_{\text{off}}$  for a single molecule. The mean event time  $\langle T_{\text{event}} \rangle$  decays exponentially with increasing applied force (Fig. 5b), following a force-dependent Arrhenius equation  $\langle T_{\text{event}} \rangle = \langle T_{\text{event}} \rangle_{F=0} \exp[-\delta F / kT]$ <sup>16</sup>. Extrapolation to zero force results in  $\langle T_{\text{event}} \rangle_{F=0} = 2.4 \pm 0.3$  s, or in an average translocated distance  $\langle L \rangle_{F=0} = \langle T_{\text{event}} \rangle_{F=0} \langle v \rangle = 1,320 \pm 150$  bp for  $R_1$  complexes.

For an  $R_2$  complex, it is not possible to use the same method to determine the time that a single motor spends translocating on DNA, because it is not clear (in most of the events) which of the two motor subunits falls off during a dissociation event after translocation activity of both motors. However, it is possible to derive the mean time that a single motor subunit spends on the DNA (see Methods). From this, we obtain  $\langle T_{\text{event}} \rangle_{F=0} = 7.7 \pm 1.6$  s and an average translocated distance of  $4,300 \pm 900$  bp per motor subunit at zero force (Fig. 5b). This is an increase of more than a factor of 3 in comparison with the  $R_1$  complex. We thus conclude that the presence of the second bound motor subunit substantially reduces the dissociation of a single motor subunit during translocation.

### Generation of twist by the motor

To produce a more detailed mechanistic picture of DNA translocation, it may help to deduce whether the motor subunits follow the helical pitch of the DNA during movement. For enzymes traveling along a single strand of double-stranded DNA, like most helicases, this must obviously be true. However, some members of the SF2 helicases, to which *EcoR124I* belongs, have been identified as double-stranded translocases<sup>13</sup>, which need not necessarily track along the helical pitch. If the HsdR subunits of *EcoR124I* follow the helical pitch of the DNA, they must reduce the number of helical turns of the translocated DNA in the loop, because the MTase is known to remain bound to the recognition site. Therefore, for each helical turn, one positive supercoil should be created ahead of the motor and one negative supercoil in the DNA loop behind. Magnetic tweezers can be used to study supercoil generation and release on single unnicked DNA molecules<sup>17</sup>. Using unnicked DNA molecules, we measured supercoil generation by the  $R_1$  complex. (Note that all experiments described so far involved

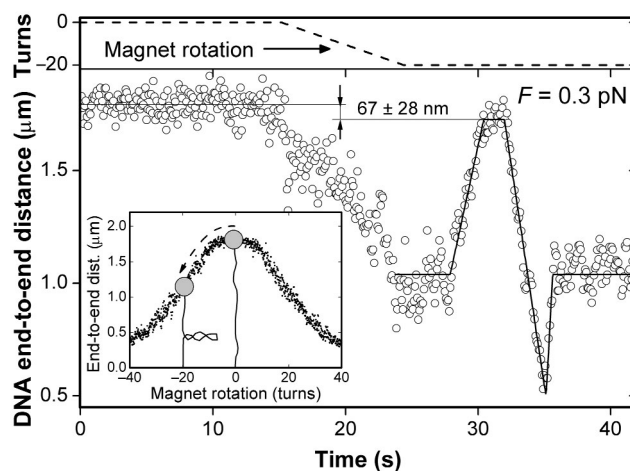
nicked DNA molecules to prevent confusion with possible reduction of the DNA end-to-end distance by plectoneme formation upon supercoiling.) By rotating the magnets, which are used to stretch the DNA, 20 negative supercoils were imposed on a DNA molecule. At forces  $<0.5$  pN, the DNA end-to-end distance then shrinks as a result of the formation of plectonemes<sup>15</sup> (Fig. 6, inset). The length decrease per generated plectoneme is  $\sim 50$  nm, as derived from the slope of the linear part of the curve in the inset. If the enzyme generates positive supercoils in the DNA ahead of it, it will, in the absence of magnet rotation, compensate the applied negative supercoils. This will remove the plectonemes, and the DNA end-to-end distance should increase rather than decrease. Indeed, the enzyme initially seems to remove the 20 negative supercoils completely and proceeds to generate about 30 positive supercoils (Fig. 6). The maximum end-to-end distance in this trace during translocation is  $67 \pm 28$  nm shorter than the DNA end-to-end distance at 0 rotations. While traveling to this point, the enzyme has depleted 20 supercoils. Therefore, the translocated distance per turn is  $3.4 \pm 1.4$  nm. Analysis of a total of five such events revealed a translocated distance of  $3.7 \pm 0.6$  nm or  $11 \pm 2$  bp per induced supercoil, in agreement with the 10.4-bp helical pitch of DNA. In all these experiments, the translocation rate of the enzyme is markedly reduced as a result of twist in the DNA molecule. For the trace shown in Figure 6, for example, the rate is  $60$  bp  $s^{-1}$ , as calculated from the time necessary to travel the 67-nm distance.

### DISCUSSION

The present study is a comprehensive single-molecule investigation of the translocation of *EcoR124I*. Beyond measuring translocation rates, we also directly measured processivity and twist generation at different assembly stages of the enzyme.

At HsdR/MTase ratios of 1:1, the measured events could clearly be attributed to the activity of a single motor subunit in accordance with the assembly of an  $R_1$  complex. The mean translocated distance at zero force was found to be  $1,320 \pm 150$  bp. Thus, the  $R_1$  complex is more than a factor of 3 less processive than the  $R_2$  complex. This confirms a previous model that assumed a reduced processivity of an  $R_1$  complex<sup>3</sup>. The translocation rate of the single motor subunit of an  $R_1$  complex was found to be  $550 \pm 30$  bp  $s^{-1}$ , in agreement with previously reported values for a high rate ( $400 \pm 32$  bp  $s^{-1}$ ) from bulk measurements<sup>3</sup>. We attribute the deviation to the better time resolution of the magnetic tweezers setup. Translocation of an  $R_2$  complex occurs

**Figure 6**  $R_1$  complex translocation on negatively supercoiled DNA (using construct I and 4 mM ATP). The DNA is supercoiled in the presence of enzyme and ATP. After random time, translocation starts and the enzyme induces positive supercoils. Therefore, plectonemes of the negative supercoiled DNA are released, resulting in an increase of the DNA end-to-end distance. At maximum position where all supercoils are released, the actual translocated distance is  $67 \pm 28$  nm. This corresponds to  $10 \pm 4$  bp traveled distance per induced supercoil, consistent with the enzyme tracking along the helical pitch. Inset: DNA end-to-end distance versus magnet rotations for the same molecule, but in the absence of enzyme. The length decrease results from the formation of plectonemes.



within experimental error with twice the rate of an  $R_1$  complex. This indicates that the two motor subunits are truly independent translocases whose forward stepping is not coordinated. This is supported by the observation that initiation of translocation is not coupled for the two HsdR subunits, because periods of single-motor activity were interspersed with periods of double-motor activity. Bidirectional movement is directly confirmed by the presence of a doubled speed. In contrast to single-molecule investigations on RecBCD helicase<sup>4</sup>, the distribution of the translocation rates for *EcoR124I* is quite narrow. This directly supports previous models used to analyze 'all or none' assays<sup>1</sup> for measuring translocation of *EcoR124I* in bulk experiments<sup>3</sup>. In that case a poissonian forward-stepping with an identical rate for the whole enzyme ensemble is assumed, in agreement with the measured narrow distribution of the translocation rates.

Notably, for the fully assembled endonuclease many stalling events at the magnetic bead are detected before cleavage occurs. However, in bulk cleavage assays, most of the DNA is cleaved within 30 s, indicating that stalling is directly followed by cleavage<sup>12</sup>. Control cleavage assays confirmed rapid DNA cleavage for the same batch of enzyme under identical enzyme concentration, as used in our single-molecule experiments (data not shown). This suggests that a magnetic bead may be less efficient at inducing cleavage than, for example, a second restriction enzyme. On the other hand, the force, which stretches the DNA, reduces the time the enzyme spends translocating the DNA (Fig. 5b). It also reduces the time the enzyme remains stalled at the magnetic bead. It might therefore reduce the probability of cleavage if the average time to induce cleavage is on the order of the average stalling time. Furthermore, force could directly affect the cleavage rate of the enzyme. The nature of the barrier that can induce rapid cleavage and the possible force dependence of cleavage require further investigation.

With this magnetic tweezers-based translocation assay, we demonstrated a new method for measuring how DNA translocation is related to the introduction of twist. Previous gel assays have shown that type I restriction enzymes induce supercoils during translocation<sup>18</sup>. Here we have shown that the supercoils generated ahead of the motor subunit of an  $R_1$  complex are specifically positive supercoils. Furthermore, the measured translocated distance of  $11 \pm 2$  bp per supercoil indicates that the motor subunit translocates along the helical pitch. This should similarly hold true for the fully assembled endonuclease, because our data show that the motor subunits of an  $R_2$  complex act independently. Notably, the enzyme was found to translocate at reduced velocity on supercoiled DNA. This could explain the reduced cleavage rate on supercoiled DNA in comparison with relaxed DNA<sup>11,12</sup>. Initially, one might guess that the torque present in supercoiled DNA molecules would slow down the enzymatic translocation rate. However, this argument applies only for positively supercoiled DNA, in which the torque opposes the DNA twisting induced by the enzyme. On negatively supercoiled DNA, the torque acts in the direction of the twist generation, which should even support the generation of positive

supercoils by the enzyme. Apparently, such a simple energetic model cannot fully explain the reduced translocation rate for supercoiled DNA. *In vivo*, the chromosomal DNA is mostly in a supercoiled state, and therefore more work is warranted to further investigate how the translocation is affected by the presence of torque.

Until now, the nature of the dissociation process, which results in termination of a translocation event, had remained unclear. The process could involve (i) dissociation of the complete endonuclease from the DNA (ii) subunit dissociation of HsdR from MTase or (iii) release of the DNA loop by the HsdR without subunit dissociation. The latter case is inconsistent with the switch of translocation direction between successive translocation events that we observed for the  $R_1$  complex. If the  $R_1$  complex remained at the DNA after translocation, one would expect it to reinitiate translocation only in the same direction, because swiveling of the motor subunit seems improbable<sup>3</sup>. Therefore, we propose that dissociation of either the whole enzyme or the HsdR subunit terminates translocation. Previous investigations have suggested that case (i), the complete detachment of the endonuclease from the DNA, does not occur<sup>19</sup>. In fact, preliminary experiments show that the time between successive events increased when lowering the HsdR/MTase ratio (R.S., J.G.P.B., N.H.D., K.F. and C.D., unpublished data), supporting the dissociation of the HsdR subunit. Such a dynamic enzyme assembly concurs with the recently reported mechanism of restriction alleviation of *EcoR124I* *in vivo*<sup>20</sup>. Thus, the dynamic behavior of assembly, translocation and disassembly that is indicated by the experiments may represent a relevant mechanism for bacterial control of DNA restriction.

The present single-molecule study is the first such report for DNA-translocating restriction enzymes. It allowed a direct confirmation of the models that were previously used to analyze kinetic data. Beyond this direct visualization of enzyme translocation, we were able to explain several issues that are difficult, if not impossible, to address in bulk measurements, for example the coupling of translocation with the generation of twist, the independent action of the two motors, and the dynamic assembly and disassembly of the enzyme during translocation.

Direct confirmation of previous translocation models for *EcoR124I*, carried out in the present study, should stimulate additional biochemical experiments, which could in combination with single-molecule data answer additional questions about, for example, the step size of the translocase, the actual cleavage mechanism and whether the enzyme tracks along double- or single-stranded DNA. Elucidating the mechanistic details of the translocation process has direct relevance for the other SF2 helicases. Finally, type I restriction enzymes may

serve as a model system to study the processes involved in twist generation by DNA-translocating enzymes at the single-molecule level.

## METHODS

**Proteins.** *EcoR124I* MTase and HsdR were purified as described<sup>12</sup>. Protein concentrations were calculated from absorbance at 280 nm using molar extinction coefficients from the literature<sup>14</sup>.  $R_1$  complexes carrying a single motor unit were formed by mixing HsdR 1:1 with MTase in buffer R (50 mM Tris-HCl, pH 8.0, 10 mM MgCl<sub>2</sub>, 1.0 mM DTT) and diluting it to 20 nM (related to the MTase concentration) in buffer R containing 4 mM ATP.  $R_2$  endonuclease was assembled at a HsdR/MTase ratio of 8:1. Cleavage activity of reconstituted  $R_2$  complexes was confirmed as published<sup>7</sup>.

**DNA constructs.** pSFV1 plasmid (Invitrogen) carrying a single *EcoR124I* site was cleaved with *SpeI* and *BamHI*, *XhoI* or *KpnI*, resulting in linear fragments with a single recognition site at 2371 bp, at 275 bp or without recognition site, respectively. These fragments were ligated to two 700-bp PCR fragments, each containing several biotin- or digoxigenin-modified UTP bases (Roche Diagnostics). Unless otherwise stated, all constructs were nicked through dephosphorylation of the biotinylated PCR fragment before ligation.

**Magnetic tweezers.** Magnetic tweezers were constructed on the basis of the system described elsewhere<sup>15</sup>. The applied force was calculated by quantifying the brownian motion of the DNA-tethered bead. Using real-time image processing, 5-nm position accuracy of the bead was obtained in all three dimensions. To exclude thermal drift, all positions were measured relative to a nonmagnetic polystyrene bead affixed to the bottom of the flow cell.

**Flow cell.** Polystyrene beads, as well as DNA constructs carrying at one end a magnetic bead, were anchored to the bottom of a flow cell as described elsewhere<sup>17</sup>. The force-extension curve of a single DNA molecule was measured. After confirmation of the correct contour and persistence lengths, experiments were started by addition of the restriction enzyme. All measurements were carried out at 25 °C.

**Data analysis.** To quantify translocation rates and distances, we fit four linear segments to each phase in the translocation cycle (Fig. 2b).

The end-to-end distance  $X$  of a DNA molecule in the magnetic tweezers is lower than the contour length  $L$  and is dependent on the applied force. Any change in the contour length, such as that due to enzyme translocation, is therefore seen in a factor of  $X/L$  (called relative extension)—reduced change of the DNA end-to-end distance. In our analysis, we corrected for this by dividing all fitted translocation distances and rates by the relative extension of the DNA at the given force.

For the  $R_2$  complex, the mean time a motor spends translocating or stalling at the DNA was calculated by the sum of all the times that the motor subunits are translocating or being stalled, divided by the number of dissociation steps. Times during which two motor subunits were active were counted twice. This can be illustrated for the time trace between 31 s and 42 s in Figure 4a: initially, two motors are translocating the DNA, after which one motor stalls while the other motor continues translocating for a time and then dissociates; the other motor remains stalled for some time until it dissociates as well. To calculate the mean time of motor activity, we summed twice the time during which both motors are translocating, twice the time during which only one motor is translocating and the other motor is stalled, and once the time the remaining motor is stalled after dissociation of the other motor. This was then divided by 2, the number of dissociation substeps. We treated stalling events similarly to

translocation events because stalling events have the same duration within error as translocation events (data not shown). Thus, the duration of both types of events is governed by the same  $k_{\text{off}}$ .

## ACKNOWLEDGMENTS

We acknowledge the financial support of the European Commission through the Mol Switch project (IST-2001-38036), of a European Molecular Biology Organization short-term fellowship to K.F., and of the Stichting voor Fundamenteel Onderzoek der Materie (FOM) and the Nederlandse Organisatie voor Wetenschappelijk Onderzoek (NWO) to C.D.

## COMPETING INTERESTS STATEMENT

The authors declare that they have no competing financial interests.

Received 13 May; accepted 14 July 2004

Published online at <http://www.nature.com/natstructmolbiol>

1. Ali, J.A. & Lohman, T.M. Kinetic measurement of the step size of DNA unwinding by *Escherichia coli* UvrD helicase. *Science* **275**, 377–380 (1997).
2. Davenport, R.J., Wuite, G.J.L., Landick, R. & Bustamante, C. Single-molecule study of transcriptional pausing and arrest by *E. coli* RNA polymerase. *Science* **287**, 2497–2500 (2000).
3. Firman, K. & Szczelkun, M.D. Measuring motion on DNA by the type I restriction endonuclease *EcoR124I* using triplex displacement. *EMBO J.* **19**, 2094–2102 (2000).
4. Bianco, P.R. *et al.* Processive translocation and DNA unwinding by individual RecBCD enzyme molecules. *Nature* **409**, 374–378 (2001).
5. Delagoutte, E. & Von Hippel, P.H. Helicase mechanisms and the coupling of helicases within macromolecular machines part I: structures and properties of isolated helicases. *Q. Rev. Biophys.* **35**, 431–478 (2002).
6. Murray, N.E. Type I restriction systems: sophisticated molecular machines (a legacy of Bertani and Weigle). *Microbiol. Mol. Biol. Rev.* **64**, 412–434 (2000).
7. Szczelkun, M.D., Janscak, P., Firman, K. & Halford, S.E. Selection of non-specific DNA cleavage sites by the type IC restriction endonuclease *EcoR124I*. *J. Mol. Biol.* **271**, 112–123 (1997).
8. Ellis, D.J., Dryden, D.T.F., Berge, T., Edwardson, J.M., & Henderson, R.M. Direct observation of DNA translocation and cleavage by the *EcoKI* endonuclease using atomic force microscopy. *Nat. Struct. Biol.* **6**, 15–17 (1999).
9. Studier, F.W. & Bandyopadhyay, P.K. Model for how type-I restriction enzymes select cleavage sites in DNA. *Proc. Natl. Acad. Sci. USA* **85**, 4677–4681 (1988).
10. Szczelkun, M.D. Kinetic models of translocation, head-on collision, and DNA cleavage by type I restriction endonucleases. *Biochemistry* **41**, 2067–2074 (2002).
11. Janscak, P., Macwilliams, M.P., Sandmeier, U., Nagaraja, V. & Bickle, T.A. DNA translocation blockage, a general mechanism of cleavage site selection by type I restriction enzymes. *EMBO J.* **18**, 2638–2647 (1999).
12. Janscak, P., Abadjieva, A. & Firman, K. The type I restriction endonuclease *R.EcoR124I*: over-production and biochemical properties. *J. Mol. Biol.* **257**, 977–991 (1996).
13. Mahdi, A.A., Briggs, G.S., Sharples, G.J., Wen, Q. & Lloyd, R.G. A model for dsDNA translocation revealed by a structural motif common to RecG and Mfd proteins. *EMBO J.* **22**, 724–734 (2003).
14. Janscak, P., Dryden, D.T.F. & Firman, K. Analysis of the subunit assembly of the type IC restriction-modification enzyme *EcoR124I*. *Nucleic Acids Res.* **26**, 4439–4445 (1998).
15. Strick, T.R., Allemand, J.F., Bensimon, D. & Croquette, V. Behavior of supercoiled DNA. *Biophys. J.* **74**, 2016–2028 (1998).
16. Howard, J. In *Mechanics of Motor Proteins and the Cytoskeleton* 88–90 (Sinauer Associates, Sunderland, Massachusetts, USA, 2001).
17. Strick, T.R., Croquette, V. & Bensimon, D. Single-molecule analysis of DNA uncoiling by a type II topoisomerase. *Nature* **404**, 901–904 (2000).
18. Janscak, P. & Bickle, T.A. DNA supercoiling during ATP-dependent DNA translocation by the type I restriction enzyme *EcoAI*. *J. Mol. Biol.* **295**, 1089–1099 (2000).
19. Endlich, B. & Linn, S. The DNA restriction endonuclease of *Escherichia coli* B. II. Further studies of the structure of DNA intermediates and products. *J. Biol. Chem.* **260**, 5729–5738 (1985).
20. Makovets, S., Powell, L.M., Titheradge, A.J.B., Blakely, G.W. & Murray, N.E. Is modification sufficient to protect a bacterial chromosome from a resident restriction endonuclease? *Mol. Microbiol.* **51**, 135–147 (2004).